JACS
JOURNAL OF THE AMERICAN CHEMICAL SOCIETY

Communication

pubs.acs.org/JACS

Synchrotron X-ray, Photoluminescence, and Quantum Chemistry Studies of Bismuth-Embedded Dehydrated Zeolite Y

Hong-Tao Sun,*[,†] Yoshitaka Matsushita,[‡] Yoshio Sakka,[§] Naoto Shirahata,[∥,⊥] Masahiko Tanaka,[‡] Yoshio Katsuya,[#] Hong Gao,[†] and Keisuke Kobayashi[‡]

[†]International Center for Young Scientists and [§]National Institute for Material Sciences (NIMS), 1-2-1 Sengen, Tsukuba-city, Ibaraki 305-0047, Japan

[‡]BL15XU, Spring-8, NIMS, and [#]SPring-8 Service Co., 1-1-1 Kohto, Sayo-cho, Hyogo 679-5148, Japan

[∥]World Premier International Research Center Initiative for Materials Nanoarchitronics, NIMS, 1-1 Namiki, Tsukuba, Ibaraki 305-0044, Japan

[⊥]PRESTO, Japan Science and Technology Agency, 4-1-8 Honcho Kawaguchi, Saitama 332-0012, Japan

Supporting Information

ABSTRACT: For the first time, direct experimental evidence of the formation of monovalent Bi (i.e., Bi^+) in zeolite Y is provided based on the analysis of high-resolution synchrotron powder X-ray diffraction data. Photoluminescence results as well as quantum chemistry calculations suggest that the substructures of Bi^+ in the sodalite cages contribute to the ultrabroad near-infrared emission. These results not only enrich the well-established spectrum of optically active zeolites and deepen the understanding of bismuth related photophysical behaviors, but also may raise new possibilities for the design and synthesis of novel hybrid nanoporous photonic materials activated by other heavier p-block elements.

Zeolites are nanoporous crystalline solids with well-defined structures containing silicon, aluminum, and oxygen in their frameworks, as well as extraframework species such as cations, water, or other molecules within their pores.[1] Owing to their microporosity, zeolites have very high surface areas and have been widely used in applications such as catalysis, ion exchange, and separations.[1] Concurrently, optically active zeolites functionalized by dyes,[2] rare-earth ions,[3−5] quantum dots,[6] and metal clusters[7] have received extensive attention owing to their great promise for creating new hybrid nanoporous materials and tremendous potential for phosphors, lasers, and biomedicines.

Bismuth is one of the most thoroughly investigated of the p-block elements; it has been called "the wonder metal" because of its diverse oxidation states and profound propensity to form clusters.[8,9] It was revealed that these subvalent Bi species ususally were stabilized by Lewis acids or exist in molecular crystals, which could show peculiar ultrawide near-infrared (NIR) photoluminescence (PL) covering the important telecommunication and biological optical windows.[9] However, although much effort has been devoted to preparing novel material systems containing such kinds of subvalent bismuth polyhedrons,[8,9] it has been rather challenging to obtain these units in traditional materials using a well-controlled and facile approach, which greatly limits their practical applications. It is believed that developing a simple and new route for obtaining the optically active bismuth centers in widely used materials such as zeolites will pave the way for their broad applications as novel broadband tunable laser media and biomarkers.

In this Communication, we provide direct experimental evidence of the formation of subvalent Bi in zeolite Y by means of synchrotron X-ray diffraction (XRD) measurements. In contrast to the common approach,[10] here we develop a well-controlled route for the preparation of optically active zeolites containing subvalent Bi, which allows the formation of NIR-active Bi while suppressing nonactive bismuth oxide agglomerates in the frameworks. For the first time, we clearly reveal that monovalent Bi (i.e., Bi^+) with a characteristic ionic radius of 1.465 Å occupies site I′ in the sodalite cage, the substructures of which contribute to the ultrabroad NIR emission. Furthermore, we rationalize the aforementioned bismuth-related photophysical behaviors through detailed quantum chemistry calculations.

Thermal treatment of Bi-embedded zeolites, with a stoichiometry $Bi_{8.5}Na_{26.6}[Al_{53.5}Si_{138.5}O_{384}]$ per unit cell, yields green powders (for experimental details, see Supporting Information (SI)). To verify whether bismuth oxide agglomerates exist in the frameworks, we examined the product through thermogravimetric (TG) analysis. Interestingly, upon rehydration, the annealed sample shows a TG curve nearly identical to that as-exchanged (Figure S1, SI), suggesting that no large clusters form in the pores of zeolites as a result of thermal treatment.

We employed high-resolution synchrotron XRD at the BL15XU NIMS beamline of SPring-8 to obtain high-quality diffraction patterns.[13] Obviously, the diffraction pattern corresponds well to the phase of zeolite Y, and no other crystalline phases appear in the final product. Crystal structure refinement by the Rietveld method has been performed using the software package GSAS (General Structure Analysis System).[14] All technical details adopted for the refinement are described in the SI. Figure 1 shows the observed and

Received: December 6, 2011
Published: January 31, 2012

   dx.doi.org/10.1021/ja211426b | J. Am. Chem. Soc. 2012, 134, 2918−2921

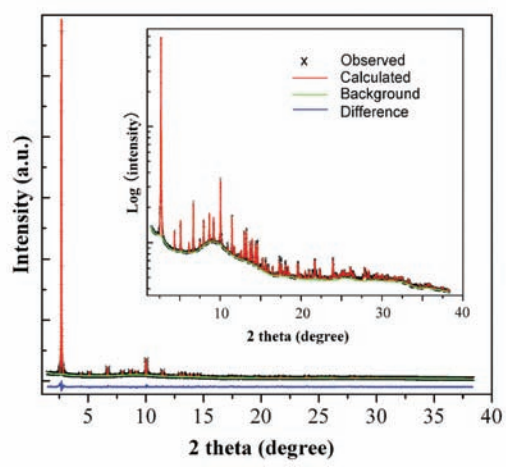

Figure 1. Rietveld fit to the high-resolution synchrotron XRD pattern of dehydrated Bi-embedded zeolite Y. Plots show the observed and calculated powder patterns. A difference curve is shown at the bottom of the diagram. Inset: a logarithmic-scale version of the graph.

calculated patterns and their intensity difference for the dehydrated zeolites. The quality of the Rietveld refinement is confirmed by the low values of R_{wp} and R_p, which are 3.14% and 2.01%, respectively. The refined cell parameter is a = 24.60237(14) Å [V = 14891.2(2) Å^3, $Fd\bar{3}m$] (see CIF file in SI).

The faujasite framework can be viewed as being built from the units of the hexagonal prism, the sodalite cavity, and the supercage. It is well recognized that cations are mainly located in a few well-defined sites, and the maximum occupancies at sites I, I′, II, II′, and III are 16, 32, 32, 32, and 48, respectively (Figure S2, SI).[11f] In the final refinement, we locate 6.9(1) Na^+ cations in site S_I, and 19.1(2) Na^+ and 8.4(0) Bi in site $S_{I'}$ (Table S1, SI), resulting in occupancy factors of 0.433(9), 0.597(5), and 0.263(1), respectively. The total amounts of Na and Bi per unit cell are 26.0(3) and 8.4(0), respectively, which agree well with those determined by ICP-OES analysis. It is necessary to note that Bi occupies a single type of site in the sodalite cages, which is coordinated to three oxygen atoms of the base of the prism.

The mean Si/Al−O bond length (1.6515 Å, see Table S2, SI) in the dehydrated sample is between the mean Si−O (1.61 Å) and Al−O (1.74 Å) distances reported for Ca-LSX (FAU).[15] In general, the oxidation states of the cations in the frameworks were assigned primarily on the basis of their ionic radii, obtained by subtracting the ionic radius of the framework oxygen (O^{2-}) from the bond length.[11f] Taking the ionic radius of O^{2-} to be 1.32 Å,[11f,16] the radius of Bi was calculated to be 1.465 Å. Further comparison of these data with the characteristic ionic radii of Bi with different oxidation states (e.g., Bi^0, 1.70 Å; Bi^+, 1.45 Å; Bi^{2+}, 1.16 Å; Bi^{3+}, 0.96 Å; and Bi^{5+}, 0.74 Å) indicates that the valence state of Bi is 1+.[17] Additionally, we found another two striking Bi^+-related features on the basis of this Rietveld refinement (Table S2). First, the Bi−Bi bond length (3.173(7) Å) is comparable to those observed in Bi polycations, of which the average Bi−Bi bond length is ∼3.1 Å.[8,9] Second, the bond angle of Bi−Bi−Bi shows an "ideal" value of 60°. These results suggest that, if Bi^+ occupies all four sites $S_{I'}$ in the sodalite cage, then ∼26.3% of the sodalite cages will contain the cluster of Bi_4^{4+}. However, owing to the low loading level, it is possible that these sites I′ are only partially occupied by Bi^+. That is, depending on the occupancy probability, Bi^+ has chances to form diverse substructures of Bi_n^{n+} (n = 1−4) in the sodalite cages, where n is the number of Bi^+ per sodalite cage (Figure S3, SI).

Next, to investigate the photophysical behaviors of the dehydrated zeolite Y containing Bi_n^{n+} (n = 1−4), we took steady-state and time-resolved PL measurements (Figure 2).

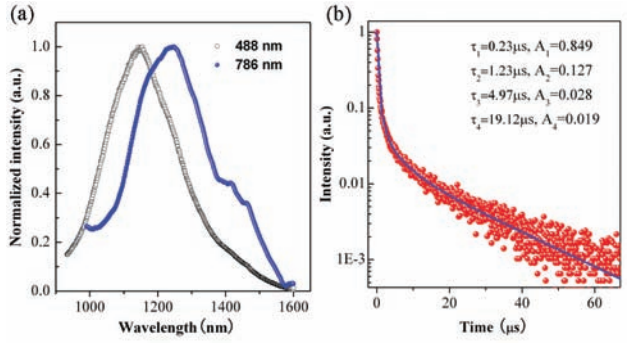

Figure 2. (a) Steady-state PL spectrum from the dehydrated sample under the excitation of 488 and 786 nm. (b) Transient emission decay profile for the above sample monitored at 1150 nm. The decay curve was fitted by $I = A_1 \exp(-t/\tau_1) + A_2 \exp(-t/\tau_2) + A_3 \exp(-t/\tau_3) + A_4 \exp(-t/\tau_4)$.

The sample displays a broad emission band from 932 to 1600 nm under the excitation of 488 nm, with a peak wavelength at 1150 nm and a full width at half-maximum of 230 nm (Figure 2a). Interestingly, the emission line shape of this sample strongly depends on the excitation wavelength; the peak wavelength shifted to 1247 nm when the sample was excited by 786 nm light. Note that under the same measurement conditions, we did not observe any PL from zeolites without bismuth, evidencing that this peculiar emission stems from the Bi_n^{n+} (n = 1−4) center. It is believed that the excitation-wavelength-dependent down-converted NIR emissions result from the coexistence of such of Bi^+ substructures in the zeolite framework. It is found that the PL from Bi_n^{n+} centers demonstrates complex multiexponential decays (Figure 2b). Clearly, the curve shows four exponential decay components, the fast initial part of which is dominant, followed by three relatively slow ones. As revealed by XRD analysis, the nearest spatial distance between adjacent Bi_n^{n+} is <1 nm. Thus, it is believed that the fastest decay is due to nonradiative cross-relaxation of active centers from the electronically excited states. However, it is difficult to make definite assignments of the slow ones, given the forbidden-like NIR transitions and overlapping of energy levels of Bi_n^{n+} centers (shown below).

To provide a deeper understanding of the origin of the PL from Bi^+-containing dehydrated zeolite Y, we performed quantum chemistry calculations using the Amsterdam Density Functional (ADF) program package developed by Baerends et al.[18] The experimentally determined geometries of Bi_n^{n+} (n = 2−4) from the XRD refinement were used for the following calculations. Spin-restricted relativistic time-dependent density functional theory (TDDFT) was employed to determine energies and compositions of excited states of these species, using the hybrid Becke three-parameter Lee−Yang−Parr (B3LYP) functional.[19] The Slater-type all-electron basis set utilized in the TDDFT calculations is of triple-ζ-polarized (TZP) quality. The absorption bands corresponding to the allowed and forbidden electronic transitions were calculated

dx.doi.org/10.1021/ja211426b | J. Am. Chem. Soc. 2012, 134, 2918−2921

through a Davidson method. The ADF numerical integration parameter was set to 4.0 in all calculations. Spin−orbit coupling was taken into account for all TDDFT calculations.

The calculated absorption spectra of Bi_4^{4+}, Bi_3^{3+} and Bi_2^{2+} in the sodalite cage are displayed in Figure 3a−c. The TDDFT

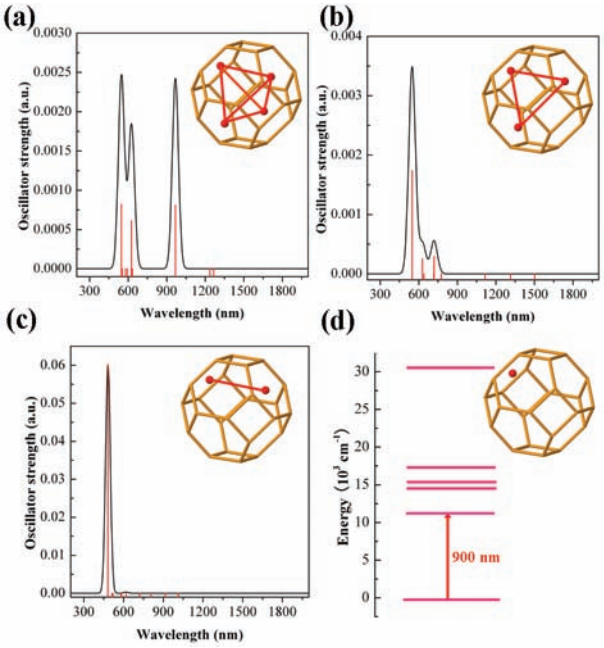

Figure 3. Theoretical absorption spectra for Bi_4^{4+} (a), Bi_3^{3+} (b), and Bi_2^{2+} (c). The red vertical lines are the oscillator strengths corresponding to specific transitions (Tables S3−S5, SI). The energy level diagram of Bi^+ (d) was drawn according to the experimental absorption spectrum of $AlCl_3$−NaCl molten salt containing Bi^+.[20e]

singlet−singlet and singlet−triplet excitation energies and oscillator strengths are compiled in Tables S3−S5 (SI). It is interesting to note that the Bi_4^{4+} unit demonstrates intense high-energy bands, with peaks at 548, 626, and 968 nm, and forbidden-like bands at 1237 and 1265 nm. Similar phenomena are also observed for Bi_3^{3+} and Bi_2^{2+} units (Figure 3b,c; Tables S4 and S5, SI). Three low-energy, forbidden-like transitions are located at 1116, 1314, and 1501 nm for Bi_3^{3+}, and at 1013, 915, and 807 nm for Bi_2^{2+}. Unfortunately, the calculation of the Bi^+ ion spectrum with the spin−orbit interaction taken into account using the present ADF software and other programs available was not successful.[22e] However, the characteristics of electronic transitions of Bi^+ could be obtained through analysis of the absorption spectrum of Bi^+ in $AlCl_3$−NaCl molten salt. It is clear that the lowest excitation energy of Bi^+ is ∼900 nm (Figure 3d).[20e] On the basis of the above results, on one hand we could conclude that all substructures of Bi^+ (i.e., Bi_4^{4+}, Bi_3^{3+}, and Bi_2^{2+}) have chances to emit in the NIR region of >930 nm. On the other hand, the large difference between these theoretical results and the experimental absorption spectrum of the dehydrated zeolites further suggests that more than one species exist in the zeolite framework (Figure S4, SI). Taken all experimental and theoretical evidence together (Figures 1−3), it is reasonable to assign the observed NIR emission to the substructures of Bi^+ in the sodalite cage of zeolite Y.

Although the synthetic approach is straightforward and leads to materials merely containing subvalent Bi as expected, the increment of Bi loading level presents a great challenge because of the higher thermal treatment temperature (see Figure S5, SI). By further optimization of the composition of zeolites used as well as the annealing temperature, it is anticipated that the sample containing only Bi_4^{4+} could be successfully obtained through the method developed here. More work is under way to prepare this kind of product and to further clarify the respective contribution of Bi^+ substructures to ultrawide NIR emission.

In summary, for the first time, we present direct experimental evidence of the formation of Bi^+ in zeolite Y through the analysis of high-resolution synchrotron powder XRD data. In combination with the results of PL and quantum chemistry calculations, we reveal that the substructures of Bi^+ residing in the sodalite cages contribute to the observed ultrabroad and tunable NIR PL. It is believed that this work will not only deepen the understanding of bismuth-related photophysical behaviors[20−22] but also raise new possibilities for the design and synthesis of novel hybrid nanoporous photonic materials using charged heavier element clusters as optically active centers, which might find broad applications for phosphors, lasers, and biomedicines.

■ ASSOCIATED CONTENT

Supporting Information

Experimental details, TG curves, Bi distribution in the sodalite cages, diffuse reflectance spectrum, tables of refined and calculated results, and CIF file of the refined XRD data. This material is available free of charge via the Internet at http://pubs.acs.org.

■ AUTHOR INFORMATION

Corresponding Author

timothyhsun@gmail.com

■ ACKNOWLEDGMENTS

H.S. gratefully acknowledges funding support from the International Center for Young Scientists, NIMS, Japan (grant no. 215114) and greatly thanks Prof. M. Fujii and Mr. Z. H. Bai (Kobe University) for support with using the PL measurement setup. The authors also thank the Materials Analysis Station, NIMS, Japan, for technical support with ICP-OES measurements.

■ REFERENCES

(1) *Zeolites and Catalysis*, 1st ed.; Čejka, J., Corma, A., Zones, S., Eds.; Wiley VCH: Berlin, 2010.

(2) (a) Pauchard, M.; Huber, S.; Méallet-Renault, R.; Maas, H.; Pansu, R.; Calzaferri, G. *Angew. Chem., Int. Ed.* **2001**, *40*, 2839. (b) Busby, M.; Kerschbaumer, H.; Calzaferri, G.; Cola, L. D. *Adv. Mater.* **2008**, *20*, 1614. (c) Brühwiler, D.; Calzaferri, G.; Torres, T.; Ramm, J. H.; Gartmann, N.; Dieu, L.; López-Duarte, I.; Martinez-Diaz, M. V. *J. Mater. Chem.* **2009**, *19*, 8040.

(3) (a) Kynast, U.; Weiler, V. *Adv. Mater.* **1994**, *6*, 937. (b) Lezhnina, M.; Laeri, F.; Benmouhadi, L.; Kynast, U. *Adv. Mater.* **2006**, *18*, 280. (c) Sun, H.; Hasegawa, T.; Fujii, M.; Shimaoka, F.; Bai, Z.; Mizuhata, M.; Hayashi, S.; Deki, S. *Appl. Phys. Lett.* **2009**, *94*, 141106. (d) Bai, Z.; Sun, H.; Hasegawa, T.; Fujii, M.; Shimaoka, F.; Miwa, Y.; Mizuhata, M.; Hayashi, S. *Opt. Lett.* **2010**, *35*, 1926.

(4) (a) Wada, Y.; Okubo, T.; Ryo, M.; Nakazawa, T.; Hasegawa, Y.; Yanagida, S. *J. Am. Chem. Soc.* **2000**, *122*, 8583. (b) Ryo, M.; Wada, Y.; Okubo, T.; Nakazawa, T.; Hasagawa, Y.; Yanagida, S. *J. Mater. Chem.* **2002**, *12*, 1748.

(5) (a) Mech, A.; Monguzzi, A.; Meinardi, F.; Mezyk, J.; Macchi, G.; Tubino, R. *J. Am. Chem. Soc.* **2010**, *132*, 4574. (b) Monguzzi, A.;

Macchi, G.; Meinardi, F.; Tubino, R.; Burger, M.; Calzaferri, G. *Appl. Phys. Lett.* **2008**, *92*, 123301. (c) Mech, A.; Monguzzi, A.; Cucinotta, F.; Meinardi, F.; Mezyk, J.; Cola, L. D.; Tubino, R. *Phys. Chem. Chem. Phys.* **2011**, *13*, 5605.
(6) (a) He, J.; Klug, D. D.; Tse, J. S.; Preston, K. F. *Chem. Commun.* **1997**, 1265. (b) Herron, N.; Wang, Y.; Eddy, M.; Stucky, G. D.; Cox, D. E.; Moller, K.; Bein, T. *J. Am. Chem. Soc.* **1989**, *111*, 530.
(7) (a) Cremer, G.; Coutiño-Gonzalez, E.; Roeffaers, M.; Moens, B.; Ollevier, J.; Auweraer, M.; Schoonheydt, R.; Jacobs, P.; De Schryver, F.; Hofkens, J.; De Vos, D.; Sels, B.; Vosch, T. *J. Am. Chem. Soc.* **2009**, *131*, 3049. (b) Cremer, G.; Coutiño-Gonzalez, E.; Roeffaers, M.; De Vos, D.; Hofkens, J.; Vosch, T.; Sels, B. *ChemPhysChem* **2010**, *11*, 1627. (c) Kim, Y.; Seff, K. *J. Am. Chem. Soc.* **1977**, *99*, 7055. (d) Kim, Y.; Seff, K. *J. Am. Chem. Soc.* **1978**, *100*, 6989. (e) Sun, T.; Seff, K. *Chem. Rev.* **1994**, *94*, 857. (f) Readman, J.; Barker, P.; Gameson, I.; Hriljac, J.; Zhou, W.; Edwards, P.; Anderson, P. *Chem. Commun.* **2004**, 736. (g) Readman, J. E.; Gameson, I.; Hriljac, J. A.; Anderson, P. *Micropor. Mespor. Mater.* **2007**, *104*, 83.
(8) (a) Krebs, B.; Hucke., M.; Brendel, C. *Angew. Chem., Int. Ed. Engl.* **1982**, *21*, 445. (b) Ulvenlund, S.; Stahl, K.; Bengtsson-Kloo, L. *Inorg. Chem.* **1996**, *35*, 223. (c) Ruck, M. *Angew. Chem., Int. Ed.* **2001**, *40*, 1182. (d) Xu, L.; Bobev, S.; El-Bahraoui, J.; Sevov, S. C. *J. Am. Chem. Soc.* **2000**, *122*, 1837. (e) Goicoechea, J. M.; Sevov, S. C. *Angew. Chem., Int. Ed.* **2006**, *45*, 5147.
(9) (a) Sun, H.; Sakka, Y.; Gao, H.; Miwa, Y.; Fujii, M.; Shirahata, N.; Bai, Z.; Li, J. *J. Mater. Chem.* **2011**, *21*, 4060. (b) Sun, H.; Sakka, Y.; Fujii, M.; Shirahata, N.; Gao, H. *Opt. Lett.* **2011**, *36*, 100.
(10) (a) Sun, H.; Hosokawa, A.; Miwa, Y.; Shimaoka, F.; Fujii, M.; Mizuhata, M.; Hayashi, S.; Deki, S. *Adv. Mater.* **2009**, *21*, 3694. (b) Sun, H.; Miwa, Y.; Shimaoka, F.; Fujii, M.; Hosokawa, A.; Mizuhata, M.; Hayashi, S.; Deki, S. *Opt. Lett.* **2009**, *34*, 1219. (c) Sun, H.; Sakka, Y.; Miwa, Y.; Shirahata, N.; Fujii, M.; Gao, H. *Appl. Phys. Lett.* **2010**, *97*, 131908.
(11) (a) Agostini, G.; Lamberti, C.; Palin, L.; Milanesio, M.; Danilina, N.; Xu, B.; Janousch, M.; van Bokhoven, J. *J. Am. Chem. Soc.* **2010**, *132*, 667. (b) Marra, G. L.; Fitch, A. N.; Zecchina, A.; Ricchiardi, G.; Salvalaggio, M.; Bordiga, S.; Lamberti, C. *J. Phys. Chem. B* **1997**, *101*, 10653. (c) Palomino, G.; Bordiga, S.; Zecchina, A.; Marra, G. L.; Lamberti, C. *J. Phys. Chem. B* **2000**, *104*, 8641. (d) Abeykoon, A.; Donner, W.; Brunelli, M.; Castro-Colin, M.; Jacobson, A. J.; Moss, S. C. *J. Am. Chem. Soc.* **2009**, *131*, 13230. (e) Abeykoon, A.; Castro-Colin, M.; Anokhina, E. V.; Iliev, M. N.; Donner, W.; Jacobson, A. J.; Moss, S. C. *Phys. Rev. B* **2008**, *77*, 075333. (f) Kim, J.; Kim, C.; Sen, D.; Heo, N.; Seff, K. *J. Phys. Chem. C* **2011**, *115*, 2750.
(12) Denisov, V. N.; Ivlev, A. N.; Lipin, A. S.; Mavrin, B. N.; Orlov, V. G. *J. Phys.: Condens. Matter* **1997**, *9*, 4967.
(13) Tanaka, M.; Katsuya, Y.; Yamamoto, A. *Rev. Sci. Instrum.* **2008**, *79*, 075106.
(14) (a) Larson, A. C.; Von Dreele, R. B. Report No. LA-UR-68-748; Los Alamos National Laboratory: Los Alamos, NM, 1987. (b) Fitch, A. N.; Marra, G. L.; Zecchina, A.; Ricchiardi, G.; Salvalaggio, M.; Bordiga, S.; Lamberti, C. Presented at 5th European Powder Diffraction Conference (EPDIC-5), Parma, Italy, May 25−28, 1997.
(15) Vitale, G.; Bull, L. M.; Morris, R. E.; Cheetham, A. K.; Toby, B. H.; Coe, C. G.; MacDougall, J. E. *J. Phys. Chem.* **1995**, *99*, 16087.
(16) Emsley, J. *The Elements*; Clarendon Press: Oxford, 1991.
(17) *User's Manual ICSD−CRYSTIN*; Bergerhoff, G.; Kilger, B.; Witthauer, C.; Hundt, R.; Sievers, R., Eds.; Institut für Anorganische Chemie der Universität: Bonn, 1986.
(18) (a) Baerends, E. J.; Ellis, D. E.; Ros, P. *Chem. Phys.* **1973**, *2*, 42. (b) Te Velde, G.; Baerends, E. J. *J. Comput. Phys.* **1992**, *99*, 84.
(19) (a) Becke, A. D. *J. Chem. Phys.* **1993**, *98*, 5648. (b) Lee, C.; Yang, W.; Parr, R. G. *Phys. Rev. B* **1988**, *37*, 785.
(20) (a) Topol, L. E.; Yosim, S. J.; Osteryoung, R. A. *J. Phys. Chem.* **1961**, *65*, 1511. (b) Boston, C. R.; Smith, G. *J. Phys. Chem.* **1962**, *66*, 1178. (c) Boston, C. R.; Smith, G. *J. Phys. Chem.* **1963**, *67*, 1849. (d) Bjerrum, N.; Boston, C. R.; Smith, G. *Inorg. Chem.* **1967**, *6*, 1162. (e) Davis, H.; Bjerrum, N.; Smith, G. *Inorg. Chem.* **1967**, *6*, 1172.
(21) (a) Meng, X.; Qiu, J. R.; Peng, M. Y.; Chen, D. P.; Zhao, Q. Z.; Jiang, X. W.; Zhu, C. S. *Opt. Express* **2005**, *13*, 1628. (b) Zhou, S. F.; Jiang, N.; Zhu, B.; Yang, H.; Ye, S.; Lakshminarayana, G.; Hao, J.; Qiu, J. *Adv. Funct. Mater.* **2008**, *18*, 1407. (c) Su, L. B.; Zhao, H.; Li, H.; Zheng, L.; Ren, G.; Xu, J.; Ryba-Romanowski, W.; Lisiecki, R.; Solarz, P. *Opt. Lett.* **2011**, *36*, 4551. (d) Peng, M. Y.; Dong, G. P.; Wondraczek, L.; Zhao, L. L.; Zhang, N.; Qiu, J. R. *J. Non-Cryst. Solids* **2011**, *357*, 2241. (e) Okhrimchuk, A.; Butvina, L.; Dianov, E.; Lichkova, N.; Zagorodnev, V.; Boldyrev, K *Opt. Lett.* **2008**, *33*, 2182. (f) Romanov, A. N.; Haula, E. V.; Fattakhova, Z. T.; Veber, A. A.; Tsvetkov, V. B.; Zhigunov, D. M.; Korchak, V. N.; Sulimov, V. B. *Opt. Mater.* **2011**, *34*, 155.
(22) (a) Sun, H.; Yang, J.; Fujii, M.; Sakka, Y.; Zhu, Y.; Asahara, T.; Shirahata, N.; Ii, M; Bai, Z.; Li, J.; Gao, H. *Small* **2011**, *7*, 199. (b) Miwa, Y.; Sun, H.; Imakita, K.; Fujii, M.; Teng, Y.; Qiu, J. R.; Sakka, Y.; Hayashi, S. *Opt. Lett.* **2011**, *36*, 4221. (c) Dai, N.; Luan, H.; Xu, B.; Yang, L.; Sheng, Y.; Liu, Z.; Li, J. J. *Non-Cryst. Solid* **2012**, *358*, 261. (d) Song, Z.; Yang, Z.; Zhou, D.; Yin, Z.; Li, C.; Wang, R.; Shang, J.; Lou, K.; Xu, Y.; Yu, X.; Qiu, J. B. J. *Lumin* **2011**, *131*, 2593. (e) Sokolov, V. O.; Plotnichenko, V. G.; Dianov, E. DOI: arXiv:1106.1519v2 [cond-mat.mtrl-sci].